Applications and Applied Mathematics: An International Journal (AAM)

Volume 16 | Issue 1 Article 19

6-2021

A High Order Finite Difference Method to Solve the Steady State Navier-Stokes Equations

Nihal J. Siriwardana
Prairie View A&M University

Saroj P. Pradhan
Prairie View A&M University

Available at
http://pvamu.edu/aam
Appl. Appl. Math.
ISSN: 1932-9466

Applications and Applied Mathematics:
An International Journal
(AAM)

Vol. 16, Issue 1 (June 2021), pp. 361 – 382

A High Order Finite Difference Method to Solve the Steady State Navier-Stokes Equations

[1*]Nihal J. Siriwardana and [2]Saroj P. Pradhan

Department of Mathematics
Prairie View A&M University
Prairie View, Texas 77446
[1]njsiriwardana@pvamu.edu, [2]sppradhan@pvamu.edu

[*]Corresponding Author

Received: April 18, 2020; Accepted: February 24, 2021

Abstract

In this article, we develop a fourth order finite difference method to solve the system of steady state Navier-Stokes equations and apply it to the benchmark problem known as the square cavity flow problem. The numerical results of u-velocity components and v-velocity components obtained at the center of the cavity are compared with the results obtained by the method developed by Greenspan and Casulli to solve the time dependent system of Navier-Stokes equations. The method described in this article is easy to implement and it has been shown to be more efficient and stable than the method by Greenspan and Casulli. Present method converges for a range of various viscosity coefficients for which the method of Greenspan and Casulli is not stable. We have included the contour plots of horizontal velocity (u) components and vertical velocity (v) components to facilitate the understanding of the steady state flow inside the cavity.

Keywords: Navier-Stokes equations; Lid-Driven cavity flow problem; Finite Difference Methods; Numerical Solution of Partial Differential Equations; Staggered grid; Non-staggered grid; Fluid flow

MSC 2010 No.: 76D05; 65M06; 35Q30

1. Introduction

The flow of an incompressible, viscous fluid can be modeled by the system of Navier-Stokes equations. The study of flow of a fluid is of such fundamental importance to design engineers and

various other scientists including numerical analysts that related numerical methods for solving Navier-Stokes equations are developed constantly.

Over the years, many numerical techniques have been developed to solve the system of Navier-Stokes equations. Among them are: the Chorin (1968), Abdallah (1987), and Greenspan and Casulli (1988). Many of the researchers who study Navier-Stokes equations do not attempt to solve the system of equations written in velocity pressure form mainly since the equations are highly non-linear and achieving convergence is a difficult task. Most of the time, researchers study the system of Navier-Stokes equations written in stream-vorticity form due to the desirable structure of the system of equations. We felt that it is high time to investigate steady state system of Navier-Stokes equations written in velocity pressure with the current fast computer facilities available.

The method developed by Greenspan and Casulli (1988) is a finite volume method defined on a staggered grid to solve the time dependent system of Navier-Stokes equations and arrive at the steady state solution. For the inquisitive reader, the theory of Navier-Stokes equations can be found in Galdi (2011). In this article, the authors assume that the reader is familiar with the staggered grid or will get accustomed to it by reading one of the references provided. The schemes derived using the staggered grid tend to be more stable than those derived using non-staggered grids. Despite the advantages, staggered mesh schemes do have drawbacks. When used with a non-rectangular flow domain and a non-uniform mesh, discretization is more difficult, especially for the non-linear terms, and a separate operator for velocity components and scalar variables such as pressure must be calculated. It is therefore suggested that if a satisfactory scheme on a non-staggered mesh can be developed, it will be more appropriate for problems involving non-uniform and non-rectangular grids.

In the following sections we show how to develop a fourth order numerical scheme defined on a non-staggered grid based on central difference approximations for the derivatives and illustrate the use of the method to solve the benchmark problem known as square cavity flow problem. Following is a brief description of square cavity flow problem and the system of steady state Navier-Stokes equations.

2. Square Cavity Flow Problem and Governing Equations

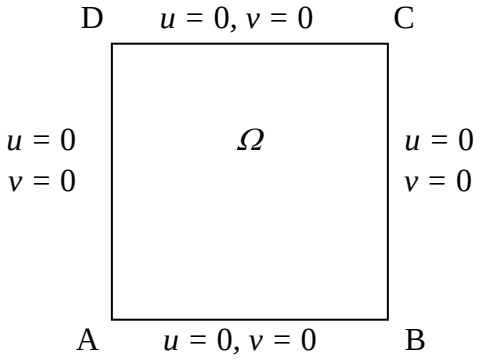

Figure 1. Cross section of square cavity with velocity boundary conditions

Let the square region Ω with vertices *A*, *B*, *C* and *D*, as shown in Figure 1, be the square cross section of a cavity. The dimensions of the square cross section are such that *AB* = *BC* = 1. The cavity is filled with an incompressible, viscous fluid and the top wall of the cavity is moving in the horizontal direction with a constant velocity $u = 1$. The motion of the top wall creates flow in the fluid, and the steady state motion of the fluid inside the cavity is governed by the system of partial differential equations shown below.

$$uu_x + vu_y + p_x - \upsilon\left(u_{xx} + u_{yy}\right) = 0\,, \tag{1a}$$
$$uv_x + vv_y + p_y - \upsilon\left(v_{xx} + v_{yy}\right) = 0\,, \tag{1b}$$
$$u_x + v_y = 0, \tag{1c}$$

where $u(x, y)$ and $v(x, y)$ are the velocity components in the X and Y directions respectively, while $p(x, y)$ is the fluid pressure and υ is kinematic viscosity which is assumed to be a constant. This system of equations is known as the system of steady state Navier-Stokes equations written in velocity pressure form.

3. Numerical Method

We place the origin of the coordinate system at point *A* on the square cavity shown in Figure 1 so that the X and Y axes will be on the AB and AD directions, respectively. We then subdivide AB into m equal parts, each of length $\Delta x = \frac{1}{m}$ by an R_{m+1} set, $x_i = (i-1)\Delta x$, $i = 1, \cdots, m+1$ and subdivide AD into n equal parts each of length $\Delta y = \frac{1}{n}$ by an R_{n+1} set, $y_j = (j-1)\Delta y$, $j = 1, \cdots, n+1$, thereby obtaining a grid containing $(m+1) \times (n+1)$ points over flow domain Ω. The u, v and p components at the grid point $\left(x_i, y_j\right)$ will be denoted by $u_{i,j}$, $v_{i,j}$ and $p_{i,j}$ respectively for $i = 1, \cdots, m+1$ and $j = 1, \cdots, n+1$.

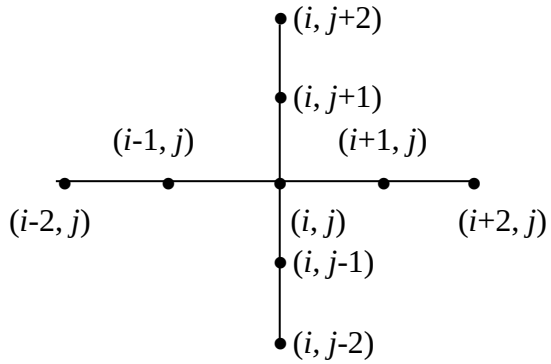

Figure 2. Nine-point grid

3.1. Difference Equations in the Interior

The partial derivatives at an interior grid point will be approximated using the 9-point grid arrangement shown in Figure 2 with fourth order central difference approximations. For example, first derivatives have been approximated using approximations of the type,

$$f_x|_{(x_i,y_j)} \approx \frac{\left(f_{i-2,j} - 8f_{i-1,j} + 8f_{i+1,j} - f_{i+2,j}\right)}{12\Delta x} + O(\Delta x^4)\,, \tag{2}$$

and second derivatives have been approximated using derivative approximations of the type,

$$f_{xx}|_{(x_i,y_j)} \approx \frac{\left(-f_{i-2,j} + 16f_{i-1,j} - 30f_{i,j} + 16f_{i+1,j} - f_{i+2,j}\right)}{12\Delta x^2} + O(\Delta x^4). \tag{3}$$

By approximating equation (1a) using the above derivative approximations, we obtain the equation,

$$u_{i,j}\left[\frac{u_{i-2,j} - 8u_{i-1,j} + 8u_{i+1,j} - u_{i+2,j}}{12\Delta x}\right] + v_{i,j}\left[\frac{u_{i,j-2} - 8u_{i,j-1} + 8u_{i,j+1} - u_{i,j+2}}{12\Delta y}\right]$$
$$+\frac{p_{i-2,j} - 8p_{i-1,j} + 8p_{i+1,j} - p_{i+2,j}}{12\Delta x} - \upsilon\left[\frac{-u_{i-2,j} + 16u_{i-1,j} - 30u_{i,j} + 16u_{i+1,j} - u_{i+2,j}}{12(\Delta x)^2}\right.$$
$$\left.+\frac{-u_{i,j-2} + 16u_{i,j-1} - 30u_{i,j} + 16u_{i,j+1} - u_{i,j+2}}{12(\Delta y)^2}\right] = 0.$$

Let $\beta = 30\upsilon\left(\frac{1}{(\Delta x)^2} + \frac{1}{(\Delta y)^2}\right)$ and apply successive over-relaxation method (SOR, it is the method of successive over-relaxation, however we had to use a relaxation factor in between 0 and 1 to achieve the convergence and hence under-relaxation) to obtain,

$$\begin{aligned} u_{i,j} = (1-\omega)u_{i,j} + \frac{\omega}{\beta}\Big[&-\left(\frac{u_{i,j}}{\Delta x} + \frac{\upsilon}{\Delta x^2}\right)u_{i-2,j} + 8\left(\frac{u_{i,j}}{\Delta x} + \frac{2\upsilon}{\Delta x^2}\right)u_{i-1,j} \\ &-8\left(\frac{u_{i,j}}{\Delta x} - \frac{2\upsilon}{\Delta x^2}\right)u_{i+1,j} \\ &-\left(-\frac{u_{i.j}}{\Delta x} + \frac{\upsilon}{\Delta x^2}\right)u_{i+2,j} - \left(\frac{v_{i,j}}{\Delta y} + \frac{\upsilon}{\Delta y^2}\right)u_{i,j-2} + 8\left(\frac{v_{i,j}}{\Delta y} + \frac{2\upsilon}{\Delta y^2}\right)u_{i,j-1} \\ &-8\left(\frac{v_{i,j}}{\Delta y} - \frac{2\upsilon}{\Delta y^2}\right)u_{i,j+1} \\ &-\left(-\tfrac{v_{i,j}}{\Delta y} + \tfrac{\upsilon}{\Delta y^2}\right)u_{i,j+2} - \tfrac{1}{\Delta x}p_{i-2,j} + \tfrac{8}{\Delta x}p_{i-1,j} - \tfrac{8}{\Delta x}p_{i+1,j} + \tfrac{1}{\Delta x}p_{i+2,j}\Big]\,, \end{aligned} \tag{4}$$

where ω is the relaxation factor and value of ω is usually in between 0 and 1. the equations we are working on are highly non-linear and we had to use under relaxing where value of ω was about 0.6 and 0.7.

We use the equation (4) to compute $u_{i,j}$ at interior grid points for $i = 3, \cdots, m-1$, $j = 3, \cdots, n-1$, in the flow domain.

By approximating equation (1b) by using above derivative approximations we obtain the equation,

$$u_{i,j}\left[\frac{v_{i-2,j}-8v_{i-1,j}+8v_{i+1,j}-v_{i+2,j}}{12\Delta x}\right]+v_{i,j}\left[\frac{v_{i,j-2}-8v_{i,j-1}+8v_{i,j+1}-v_{i,j+2}}{12\Delta y}\right]$$
$$+\frac{p_{i,j-2}-8u_{i,j-1}+8p_{i,j+1}-p_{i,j+2}}{12\Delta y}-v\left[\frac{-v_{i-2,j}+16v_{i-1,j}-30v_{i,j}+16v_{i+1,j}-v_{i+2,j}}{12(\Delta x)^2}\right.$$
$$\left.+\frac{-v_{i,j-2}+16v_{i,j-1}-30v_{i,j}+16v_{i,j+1}-v_{i,j+2}}{12(\Delta y)^2}\right]=0.$$

Let $\beta=30v\left(\frac{1}{(\Delta x)^2}+\frac{1}{(\Delta y)^2}\right)$ and apply SOR method to obtain,

$$\begin{aligned}v_{i,j}=(1-\omega)v_{i,j}+\frac{\omega}{\beta}\Big[&-\left(\frac{u_{i,j}}{\Delta x}+\frac{v}{\Delta x^2}\right)v_{i-2,j}+8\left(\frac{u_{i,j}}{\Delta x}+\frac{2v}{\Delta x^2}\right)v_{i-1,j}\\&-8\left(\frac{u_{i,j}}{\Delta x}-\frac{2v}{\Delta x^2}\right)v_{i+1,j}\\&-\left(-\frac{u_{i,j}}{\Delta x}+\frac{v}{\Delta x^2}\right)v_{i+2,j}-\left(\frac{v_{i,j}}{\Delta y}+\frac{v}{\Delta y^2}\right)v_{i,j-2}+8\left(\frac{v_{i,j}}{\Delta y}+\frac{2v}{\Delta y^2}\right)v_{i,j-1}\\&-8\left(\frac{v_{i,j}}{\Delta y}-\frac{2v}{\Delta y^2}\right)v_{i,j+1}\\&-\left(-\frac{v_{i,j}}{\Delta y}+\frac{v}{\Delta y^2}\right)v_{i,j+2}-\frac{1}{\Delta y}p_{i,j-2}+\frac{8}{\Delta y}p_{i,j-1}-\frac{8}{\Delta y}p_{i,j+1}+\frac{1}{\Delta y}p_{i,j+2}\Big].\end{aligned}\tag{5}$$

We use equation (5) to compute $v_{i,j}$ for $i=3,\cdots,m-1$, $j=3,\cdots,n-1$.

By approximating equation (1c) using central difference approximations, we obtain,

$$\frac{u_{i-2,j}-8u_{i-1,j}+8u_{i+1,j}-u_{i+2,j}}{12\Delta x}+\frac{v_{i,j-2}-8v_{i,j-1}+8v_{i,j+1}-v_{i,j+2}}{12\Delta y}=0.$$

Multiplying by 12 and separating terms we obtain,

$$\frac{u_{i-2,j}}{\Delta x}-8\frac{u_{i-1,j}}{\Delta x}+8\frac{u_{i+1,j}}{\Delta x}-\frac{u_{i+2,j}}{\Delta x}+\frac{v_{i,j-2}}{\Delta x}-8\frac{v_{i,j-1}}{\Delta x}+8\frac{v_{i,j+1}}{\Delta x}-\frac{v_{i,j+2}}{\Delta x}=0.\tag{6}$$

We then construct $u_{i-2,j}$, $u_{i-1,j}$, $u_{i+1,j}$ and $u_{i+2,j}$ from equation (4), $v_{i,j-2}$, $v_{i,j-1}$, $v_{i,j+1}$ and $v_{i,j+2}$ from equation (5) and substitute them in equation (6). The resulting equation will have the form

$$\alpha p_{i,j}+\gamma=0,\tag{7}$$

where $p_{i,j}$ is the pressure at the interior point (x_i,y_j), α is the coefficient of the $p_{i,j}$ term and γ are the rest of the terms in the equation.

It can be shown that

$$\alpha = \frac{1}{\beta(\Delta x)^2} + \frac{64}{\beta(\Delta x)^2} + \frac{64}{\beta(\Delta x)^2} + \frac{1}{\beta(\Delta x)^2} + \frac{1}{\beta(\Delta y)^2} + \frac{64}{\beta(\Delta y)^2} + \frac{64}{\beta(\Delta y)^2} + \frac{1}{\beta(\Delta y)^2} .$$

By substituting for β and simplifying further we obtain,

$$\alpha = \frac{130}{\beta(\Delta x)^2} + \frac{130}{\beta(\Delta y)^2} = \frac{130}{30\upsilon\left(\frac{1}{(\Delta x)^2} + \frac{1}{(\Delta y)^2}\right)}\left(\frac{1}{(\Delta x)^2} + \frac{1}{(\Delta y)^2}\right) = \frac{13}{3\upsilon} .$$

.

By applying the method of relaxation to equation (7) we obtain,

$$p_{i,j} = p_{i,j} - \frac{\omega}{\alpha}\left(\alpha p_{i,j} + \gamma\right), \tag{8}$$

where ω is the relaxation factor and $0 < \omega < 1$.

Since

$$\frac{u_{i-2,j} - 8u_{i-1,j} + 8u_{i+1,j} - u_{i+2,j}}{\Delta x} + \frac{v_{i,j-2} - 8v_{i,j-1} + 8v_{i,j+1} - v_{i,j+2}}{\Delta y} = \alpha p_{i,j} + \gamma ,$$

substituting for

$$\alpha\, p_{i,j} + \gamma ,$$

and α in equation (8) and simplifying we obtain the following equation for computing pressure $p_{i,j}$ at an interior point $\left(x_i, y_j\right)$.

$$p_{i,j} = p_{i,j} - \frac{3\upsilon\omega}{13}\left[\frac{u_{i-2,j} - 8u_{i-1,j} + 8u_{i+1,j} - u_{i+2,j}}{\Delta x} + \frac{v_{i,j-2} - 8v_{i,j-1} + 8v_{i,j+1} - v_{i,j+2}}{\Delta y}\right].$$

. (9)

Equation (9) is used to compute the pressure p at an interior point $\left(x_i, y_j\right)$, where $i = 3, \cdots, m-1$, $j = 3, \cdots, n-1$.

3.2. Inner Boundary

The square consisting of grid lines one step inside each wall (inner boundary) is defined as the inner boundary. (Part of inner boundary close to left vertical wall is shown in Figure 3). In order to use equations (4) and (5) to compute the velocity components at the grid points on the inner boundary, we need fictitious u and v velocity components as well as a fictitious p pressure. For example, to compute $u_{2,j}$ using equation (4) or $v_{2,j}$ using equation (5), fictitious velocity components $u_{0,j}$ and fictitious pressure $p_{0,j}$ are needed.

Neither the p values nor any derivative conditions on the boundary are known. Thus, we construct a different set of equations to compute u, v and p along the inner boundary. This section illustrates the development of relevant equations on the left side of the inner boundary.

We approximate the equation (1a) using derivative approximations such as

$$f_x|_{(x_i,y_j)} \approx \frac{\left(-3f_{i-1,j} - 10f_{i,j} + 18f_{i+1,j} - 6f_{i+2,j} + f_{i+3,j}\right)}{12\Delta x} + O(\Delta x^4), \tag{10}$$

and

$$f_{xx}|_{(x_i,y_j)} \approx \frac{\left(10f_{i-1,j} - 15f_{i,j} - 4f_{i+1,j} + 14f_{i+2,j} - 6f_{i+3,j} + f_{i+4,j}\right)}{12\Delta x^2} + O(\Delta x^4), \tag{11}$$

for the derivatives with respect to variable x and central difference approximations for the derivatives with respect to variable y.

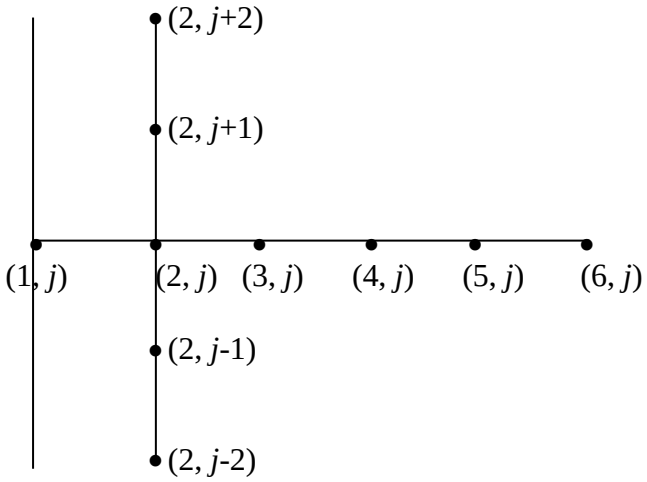

Figure 3. Left Inner Boundary

We then apply SOR to obtain the following equation,

$$\begin{aligned} u_{i,j} = (1-\omega)u_{i,j} + \frac{\omega}{\beta_2}\Bigg[u_{i,j}\left(\frac{-3u_{i-1,j} - 10u_{i,j} + 18u_{i+1,j} - 6u_{i+2,j} + u_{i+3,j}}{\Delta x}\right) \\ + v_{i,j}\left(\frac{u_{i,j-2} - 8u_{i,j-1} + 8u_{i,j+1} - u_{i,j+2}}{\Delta y}\right) + \frac{-3p_{i-1,j} - 10p_{i,j} + 18p_{i+1,j} - 6p_{i+2,j} + p_{i+3,j}}{\Delta x} \\ - v\left(\frac{10u_{i-1,j} - 4u_{i+1,j} + 14u_{i+2,j} - 6u_{i+3,j} + u_{i+4,j}}{(\Delta x)^2} + \frac{-u_{i,j-2} + 16u_{i,j-1} + 16u_{i,j+1} - u_{i,j+2}}{(\Delta y)^2}\right)\Bigg], \end{aligned} \tag{12}$$

where $\beta_2 = \upsilon\left(\frac{15}{(\Delta x)^2} + \frac{30}{(\Delta y)^2}\right)$. We use equation (12) to compute the u velocity component for $i = 2,\ j = 3, \cdots, n-1$.

Similarly, by approximating equation (1b) using appropriate derivatives and applying SOR, one can develop the following equation for computing v velocity components along the left inner boundary.

$$v_{i,j} = (1-\omega)v_{i,j} + \frac{\omega}{\beta_2}\left[u_{i,j}\left(\frac{-3v_{i-1,j} - 10v_{i,j} + 18v_{i+1,j} - 6v_{i+2,j} + v_{i+3,j}}{\Delta x}\right)\right.$$
$$+v_{i,j}\left(\frac{v_{i,j-2} - 8v_{i,j-1} + 8v_{i,j+1} - v_{i,j+2}}{\Delta y}\right) + v_{i,j}\left(\frac{p_{i,j-2} - 8p_{i,j-1} + 8p_{i,j+1} - p_{i,j+2}}{\Delta y}\right)$$
$$\left.-\upsilon\left(\frac{10v_{i-1,j} - 4v_{i+1,j} + 14v_{i+2,j} - 6v_{i+3,j} + v_{i+4,j}}{(\Delta x)^2} + \frac{-v_{i,j-2} + 16v_{i,j-1} + 16v_{i,j+1} - v_{i,j+2}}{(\Delta y)^2}\right)\right], \tag{13}$$

where β_2 is same as in equation (12) and we use equation (13) to compute the v-velocity component for $i = 2, j = 3, \cdots, n-1$.

Now to develop an equation to compute pressure at grid points $p_{2,j}$ where $j = 3, \cdots, n-1$, we construct $u_{i-2,j}$, $u_{i-1,j}$, $u_{i+1,j}$and $u_{i+2,j}$ from equation (12) and $v_{i,j-2}$, $v_{i,j-1}$, $v_{i,j+1}$ and $v_{i,j+2}$ from equation (13) and substitute them in equation (6). Then we combine all the terms and pick a coefficient (say α_1) of $p_{i,j}$.

We find that $\alpha_1 = \frac{174}{\beta_2(\Delta x)^2} + \frac{130}{\beta_2(\Delta y)^2}$. We then construct the following equation (14) to compute $p_{2,j}$ for $j = 3, \cdots, n-1$.

$$p_{2,j} = p_{2,j} - \frac{\omega}{\alpha_1}\left[\frac{u_{0,j} - 8u_{1,j} + 8u_{3,j} - u_{4,j}}{\Delta x} + \frac{v_{2,j-2} - 8v_{2,j-1} + 8v_{2,j+1} - v_{2,j+2}}{\Delta y}\right]. \tag{14}$$

Equation (14) requires a fictitious u velocity component $u_{0,j}$, $(j = 3, \cdots, n-1)$ which is outside the left vertical boundary. The method of construction of $u_{0,j}$ is illustrated below.

3.3. Fictitious $u_{0,j}$

We first construct the cubic interpolation polynomial using the points $(1,j)$, $(2,j)$, $(3,j)$ and $(4,j)$, and then extrapolate it to obtain the fictitious $u_{0,j}$ as shown below.

$$u(x) = a + bx + cx^2 + dx^3.$$

Since $u_{1,j} = 0$, by substituting the ordered pair $(0, u_{1,j})$, we obtain $a = 0$.

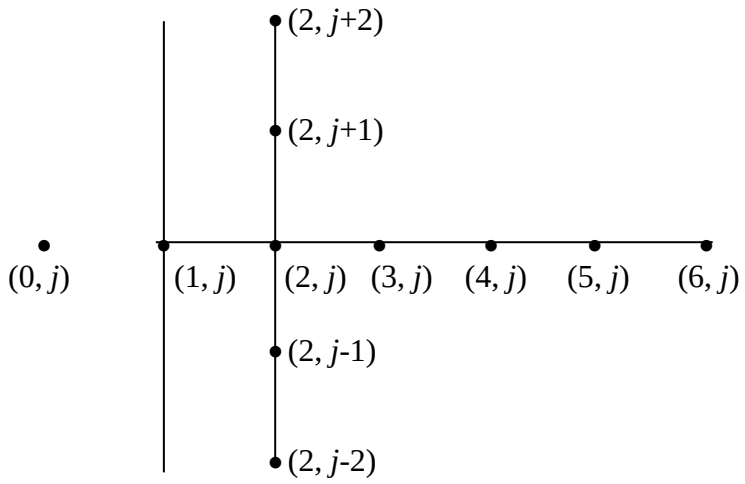

Figure 4. Fictitious point (0, *j*)

By substituting $(\Delta x, u_{2,j})$, $(2\Delta x, u_{3,j})$ and $(3\Delta x, u_{4,j})$ we obtain the following system of equations for unknowns b, c and d.

$$\Delta x b + (\Delta x)^2 c + (\Delta x)^3 d = u_{2,j},$$

$$2\Delta x b + 4(\Delta x)^2 c + 8(\Delta x)^3 d = u_{3,j},$$

$$3\Delta x b + 9(\Delta x)^2 c + 27(\Delta x)^3 d = u_{4,j}.$$

By solving this system, we obtain,

$$b = \frac{1}{6\Delta x}\left(18u_{2,j} - 9u_{3,j} + 2u_{4,j}\right),$$

$$c = -\frac{1}{2(\Delta x)^2}\left(5u_{2,j} - 4u_{3,j} + u_{4,j}\right),$$

$$d = \frac{1}{6(\Delta x)^3}\left(3u_{2,j} - 3u_{3,j} + u_{4,j}\right).$$

Now by substituting the pair $(-\Delta x,\ u_{0,j})$ we obtain $u_{0,j} = -b(\Delta x) + c(\Delta x)^2 - d(\Delta x)^3$ for $j = 2, \cdots, n$. A similar construction is used to obtain the fictitious u velocity $u_{m+2,j}$, $j = 2, \cdots, n$, outside the right boundary.

3.4. Fictitious velocity $v_{i,n+2}$

We first construct the cubic polynomial $v(y) = a + by + cy^2 + dy^3$ using the points $(1, v_{i,n+1})$, $(1-\Delta y, v_{i,n})$, $(1-2\Delta y, v_{i,n-1})$ and $(1-3\Delta y, v_{i,n-2})$, and use this polynomial to obtain the fictitious $u_{i,n+2}$ as shown below.

By substituting the above points in the polynomial, we obtain the following system of equations.

$$\begin{cases} a+b+c+d=0\,, \\ a+(1-\Delta y)b+(1-\Delta y)^2c+(1-\Delta y)^3d=v_{i,n}\,, \\ a+(1-2\Delta y)b+(1-2\Delta y)^2c+(1-2\Delta y)^3d=v_{i,n-1}\,, \\ a+(1-3\Delta y)b+(1-3\Delta y)^2c+(1-3\Delta y)^3d=v_{i,n-2}\,. \end{cases}$$

By solving the above system, we obtain the following values for coefficients of the polynomial.

$$a=-\frac{1}{6(\Delta y)^3}[-3(1-5\Delta y+6(\Delta y)^2)v_{i,n}+3(1-4\Delta y+3(\Delta y)^2)v_{i,n-1} -(1-3\Delta y+2(\Delta y)^2)v_{i,n-2}]\,,$$

$$b=-\frac{1}{6(\Delta y)^3}[3(3-10\Delta y+6(\Delta y)^2)v_{i,n}-3(3-8\Delta y+3(\Delta y)^2)v_{i,n-1} +(3-6\Delta y+2(\Delta y)^2)v_{i,n-2}\,,$$

$$c=-\frac{1}{2(\Delta y)^3}\left[(-3+5\Delta y)v_{i,n}+(3-4\Delta y)v_{i,n-1}+(-1+\Delta y)v_{i,n-2}\right],$$

$$d=-\frac{1}{6(\Delta y)^3}\left[-3v_{i,n}-3v_{i,n-1}+v_{i,n-2}\right].$$

We then use the equation $v_{i,n+2}=a+b(1+\Delta y)+c(1+\Delta y)^2+d(1+\Delta y)^3$ for $i=2,\cdots,m$ and a similar construction is used to obtain the fictitious v velocity $v_{i,0}$, $i=2,\cdots,m$ just outside the bottom boundary.

3.5. Corner Point (2, *n*)

To compute the velocities and pressure at corner points on the inner boundary we develop special equations. The derivation of difference equations for velocity and pressure at the corner point $(2,n)$ is shown below.

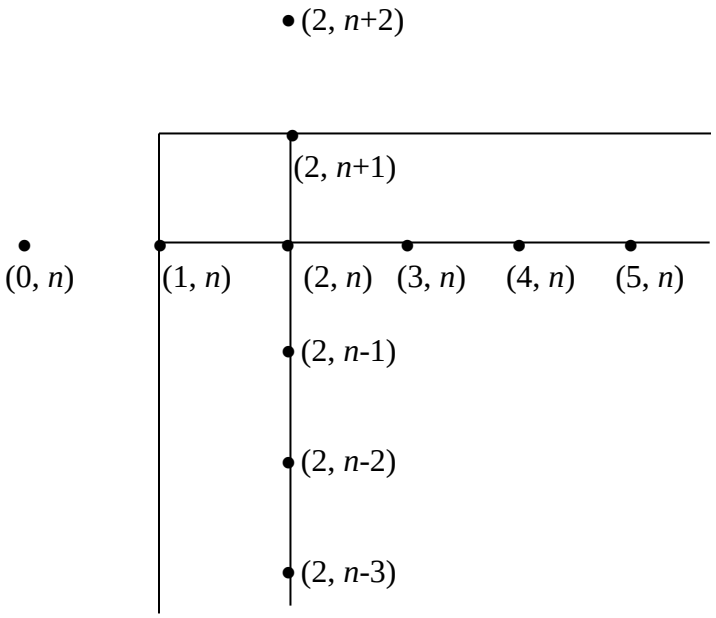

Figure 5. Corner Point (2, *n*)

We approximate equation (1a) to obtain,

$$u_{i,j}\left[\frac{-3u_{i-1,j}-10u_{i,j}+18u_{i+1,j}-6u_{i+2,j}+u_{i+3,j}}{12\Delta x}\right]+v_{i,j}\left[\frac{-3u_{i,j-3}+6u_{i,j-2}-18u_{i,j-1}+10u_{i,j}+3u_{i,j+1}}{12\Delta y}\right]+\frac{-3p_{i-1,j}-10p_{i,j}+18p_{i+1,j}-6p_{i+2,j}+p_{i+3,j}}{12\Delta x}-v\left[\frac{10u_{i-1,j}-15u_{i,j}-4u_{i+1,j}+14u_{i+2,j}-6u_{i+3,j}+u_{i+4,j}}{12(\Delta x)^2}+\frac{u_{i,j-4}-6u_{i,j-3}+14u_{i,j-2}-4u_{i,j-1}-15u_{i,j}+10u_{i,j+1}}{12(\Delta y)^2}\right]=0\,.$$

By applying SOR, we obtain,

$$u_{i,j}=(1-\omega)u_{i,j}+\frac{\omega}{\beta_3}\left[u_{i,j}\left(\frac{-3u_{i-1,j}-10u_{i,j}+18u_{i+1,j}-6u_{i+2,j}+u_{i+3,j}}{\Delta x}\right)+v_{i,j}\left(\frac{-u_{i,j-3}+6u_{i,j-2}-18u_{i,j-1}+10u_{i,j}+3u_{i,j+1}}{\Delta y}\right)+\frac{-3p_{i-1,j}-10p_{i,j}+18p_{i+1,j}-6p_{i+2,j}+p_{i+3,j}}{\Delta x}\right.$$

$$-\upsilon\left(\frac{10u_{i-1,j}-4u_{i+1,j}+14u_{i+2,j}-6u_{i+3,j}+u_{i+4,j}}{(\Delta x)^2}\right.$$

$$\left.+\frac{u_{i,j-4}-6u_{i,j-3}+14u_{i,j-2}-4u_{i,j-1}+10u_{i,j+1}}{(\Delta x)^2}\right)], \tag{15}$$

where $\beta_3 = 15\upsilon\left(\frac{1}{(\Delta x)^2}+\frac{1}{(\Delta y)^2}\right)$. We use equation (15) to compute $u_{2,n}$.

Similarly, one can develop the equation,

$$v_{i,j} = (1-\omega)v_{i,j} - \frac{1}{\beta_3}[u_{i,j}\left(\frac{-3v_{i-1,j}-10v_{i,j}+18v_{i+1,j}-6v_{i+2,j}+v_{i+3,j}}{\Delta x}\right)$$

$$+v_{i,j}\left(\frac{-v_{i,j-3}+6v_{i,j-2}-18v_{i,j-1}+10v_{i,j}+3v_{i,j+1}}{\Delta y}\right)$$

$$+\frac{-p_{i,j-3}+6p_{i,j-2}-18p_{i,j-1}+10p_{i,j}+3p_{i,j+1}}{\Delta y}$$

$$-\upsilon\left(\frac{10v_{i-1,j}-4v_{i+1,j}+14v_{i+2,j}-6v_{i+3,j}+v_{i+4,j}}{(\Delta x)^2}\right.$$

$$\left.+\frac{v_{i,j-4}-6v_{i,j-3}+14v_{i,j-2}-4v_{i,j-1}+10v_{i,j+1}}{(\Delta y)^2}\right)], \tag{16}$$

where $\beta_3 = 15\upsilon\left(\frac{1}{(\Delta x)^2}+\frac{1}{(\Delta y)^2}\right)$. We use equation (16) to compute $v_{2,n}$.

We then construct $u_{i-2,j}$, $u_{i-1,j}$, $u_{i+1,j}$ and $u_{i+2,j}$ from equation (15), $v_{i,j-2}$, $v_{i,j-1}$, $v_{i,j+1}$ and $v_{i,j+2}$ from equation (16) and substitute them in equation (6). Let α_2 be the coefficient of $p_{i,j}$, of the resulting equation. It can be shown that

$$\alpha_2 = \frac{174}{\beta_3(\Delta x)^2}+\frac{174}{\beta_3(\Delta y)^2} = \frac{58}{5\upsilon},$$

and the following equation is obtained for computing pressure at the corner point $(2,n)$.

$$p_{2,n} = p_{2,n} - \frac{5\upsilon\omega}{58}\left[\frac{u_{0,n}-8u_{1,n}+8u_{3,n}-u_{4,n}}{\Delta x}+\frac{v_{2,n-2}-8v_{2,n-1}+8v_{2,n+1}-v_{2,n+2}}{\Delta y}\right].$$

This equation uses the fictitious velocity values $u_{0,n}$ and $v_{2,n+2}$ we have already constructed.

3.6. The Difference Equations at the Boundary

Velocity components on the boundary walls are known. To approximate the unknown pressure on the boundary walls, we construct four different approximations. The following illustrates the construction of the equations to compute the pressure on the left wall.

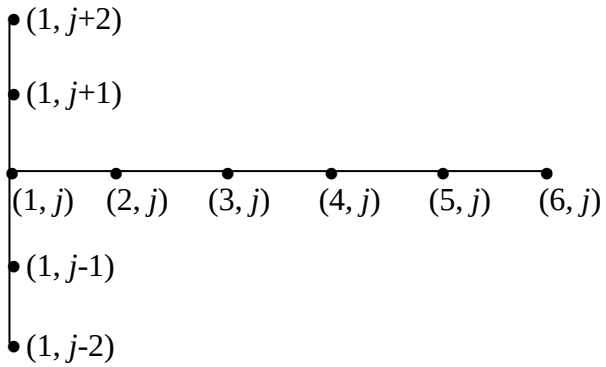

Figure 6. Left Boundary

Since $u = 0$ and $v = 0$ along the left boundary, equation (1a) reduces to

$$p_x - \upsilon\left(u_{xx} + u_{yy}\right) = 0\,. \tag{17}$$

We approximate equation (17) using the grid points shown in Figure 6 and derivative approximations of the type

$$f_x|_{(x_i,y_j)} \approx \frac{\left(-25f_{i,j} + 48f_{i+1,j} - 36f_{i+2,j} + 16f_{i+3,j} - 3f_{i+4,j}\right)}{12\Delta x} + O(\Delta x^4)$$

and

$$f_{xx}|_{(x_i,y_j)} \approx \frac{225f_{i,j} - 770f_{i+1,j} + 1070f_{i+2,j} - 780f_{i+3,j} + 305f_{i+4,j} - 50f_{i+5,j}}{60(\Delta x)^2} + O(\Delta x^4)$$

to obtain,

$$\frac{-25p_{1,j} + 48p_{2,j} - 36p_{3,j} + 16p_{4,j} - 3p_{5,j}}{12\Delta x}$$

$$-\upsilon\left(\frac{225u_{1,j} - 770u_{2,j} + 1070u_{3,j} - 780u_{4,j} + 305u_{5,j} - 50u_{6,j}}{60(\Delta x)^2}\right) = 0.$$

After simplifying we obtain,

$$-25p_{1,j} + 48p_{2,j} - 36p_{3,j} + 16p_{4,j} - 3p_{5,j} - \frac{\upsilon}{\Delta x}(-154u_{2,j} + 214u_{3,j} - 156u_{4,j} + 61u_{5,j} - 10u_{6,j}) = 0.$$

We then apply the method of relaxation to the above equation to obtain the pressure along the left vertical boundary. Similar approximations are used to compute the pressure along the other boundaries.

4. Numerical Results

Table 1 and Table 2 contain u velocity components and v velocity components obtained from the present method developed in the paper at the center of the cavity, (0.5, 0.5), and those obtained from the method by Greenspan and Casulli. We used the tolerance value of $\varepsilon = 0.0000005$ with each of the grid sizes provided in the tables. The computer program was stopped when the absolute difference between successive u, v and p became smaller than ε. We used under relaxing for each of the grid sizes tested, with a relaxation factor of $\omega = 0.7$ or $\omega = 0.6$.

The results obtained by the present method are found to be in good agreement with those of Greenspan and Casulli (1988). The values in the table show that the present method converges towards the solution faster than the staggered grid method of Greenspan and Casulli. The present method can produce results with a coarser grid, such as 20×20, for larger values of the kinematic viscosity coefficient such as $v = 0.01$. This is expected since the present method is fourth order in the interior as well as on the boundary, whereas method by Greenspan and Casulli (1988) approximate the partial derivatives of velocity components and pressure using second order central difference approximations.

We tested the method by Greenspan and Casulli (1988) for the viscosity coefficient of $\upsilon = 0.01$, but we were unable to achieve convergence for a 320×320 grid due to the long computing time involved and the tedious task of selecting appropriate parameters for each test run of the simulation. Hence, we included the values obtained by Richardson extrapolation to facilitate the comparison. We observed that the time required for the present method to reach the steady state solution is about 1/25 of the time required by Greenspan and Casulli (1988) for a 160×160 grid.

Note that the results obtained for $\upsilon = 0.01$ by the present method for the 160×160 case are the same as the extrapolated results obtained by the method of Greenspan and Casulli. Also, if we apply extrapolation to results obtained with 40×40 and 80×80 grids, we obtain the extrapolated results obtained by Greenspan and Casulli.

Table 1. Values of u-velocity components and the v-velocity components at the center of the cavity for $\upsilon = 0.01$

Value of υ	Reference	Grid Size	u at center (0.5,0.5)	v at center (0.5,0.5)
0.01	Method by Greenspan	40 × 40	−0.20496	0.05669
		80 × 80	−0.20812	0.05732
		160 × 160	−0.20888	0.05749
		Extrapolated	−0.20913	0.05755
0.01	Present Method	20 × 20	−0.20123	0.05027
		40 × 40	−0.20848	0.05688
		80 × 80	−0.20907	0.05748
		160 × 160	−0.20913	0.05753
		320 × 320	−0.20914	0.05753

Table 2. Values of u-velocity components and the v-velocity components at the center of the cavity obtained by the present method for $\upsilon = 0.005, \upsilon = 0.002$ and $\upsilon = 0.001$

Value of υ	Reference	Grid Size	u at center (0.5, 0.5)	v at center (0.5, 0.5)
0.005	Present Method	40 × 40	-0.198536	0.082400
		80 × 80	-0.198147	0.083565
		100 × 100	-0.198709	0.083620
0.002	Present Method	40 × 40	-0.104454	0.041850
		80 × 80	-0.096192	0.041011
		100 × 100	-0.095602	0.041276
0.001	Present Method	40 × 40	N/A	N/A
		80 × 80	N/A	N/A
		100 × 100	-0.062307	0.025797
		160 × 160	-0.061903	0.025757

We were not able to achieve convergence using the method of Greenspan and Casulli with smaller viscosity coefficients such as $\upsilon = 0.005$, $\upsilon = 0.002$ and $\upsilon = 0.001$. However, the present method did converge for those viscosity coefficients, and the results are shown in Table 2.

Achieving convergence for viscosity coefficients smaller than $\upsilon = 0.002$ was difficult with a coarser grid. However, since we could achieve convergence with a 100×100 grid for all the viscosity coefficients we tried, a grid of size 100×100 was used to construct contour graphs of u-velocity and v-velocity components.

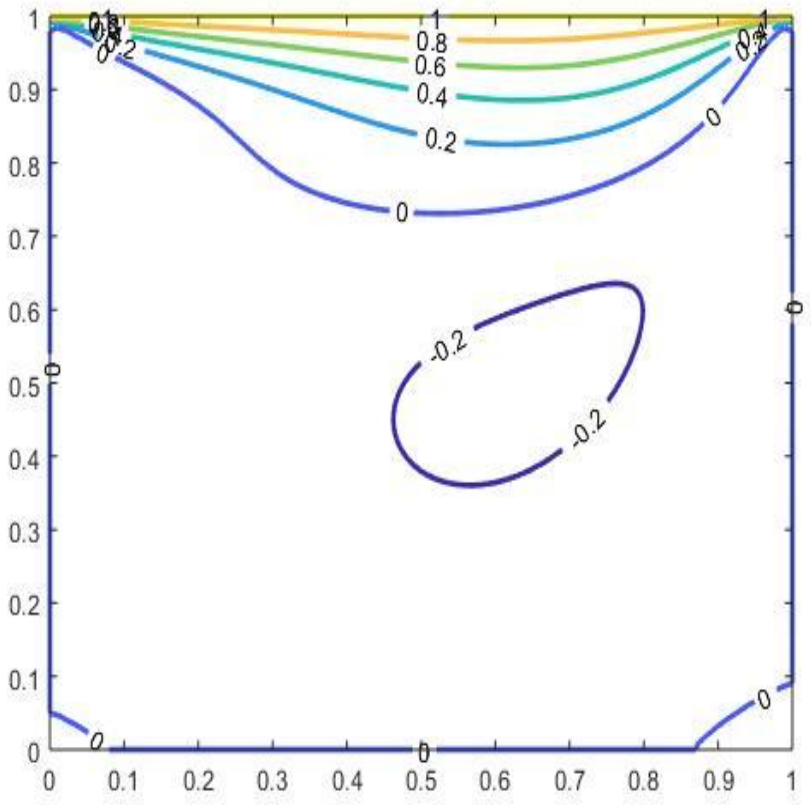

Figure 7. 2D u-velocity contours with various levels for $\upsilon = 0.01$. Grid size 100x100

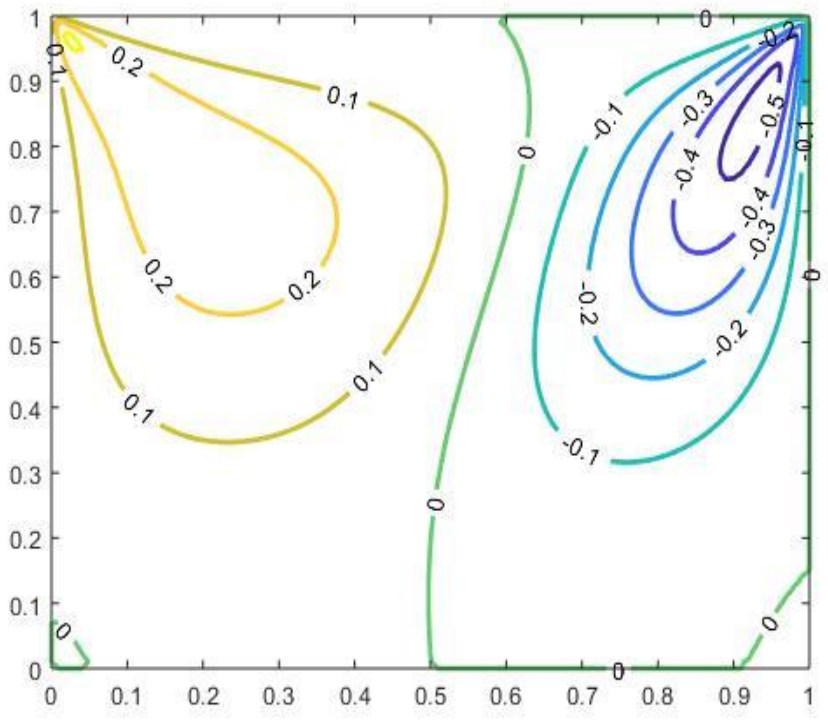

Figure 8. 2D v-velocity contours with various levels for $\upsilon = 0.01$. Grid size 100x10

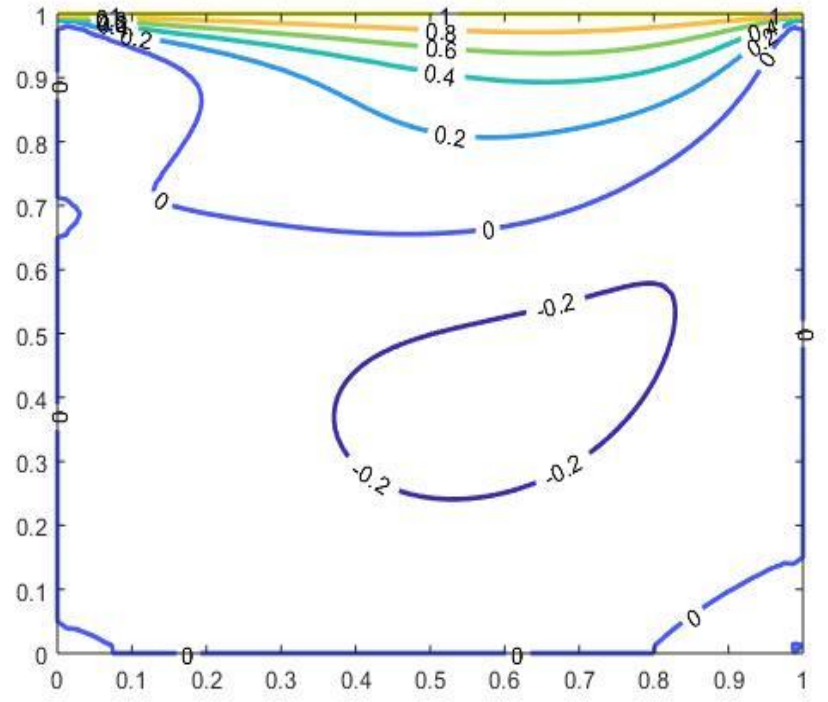

Figure 9. 2D u-velocity contours with various levels for $\upsilon = 0.005$. Gid size 100x100

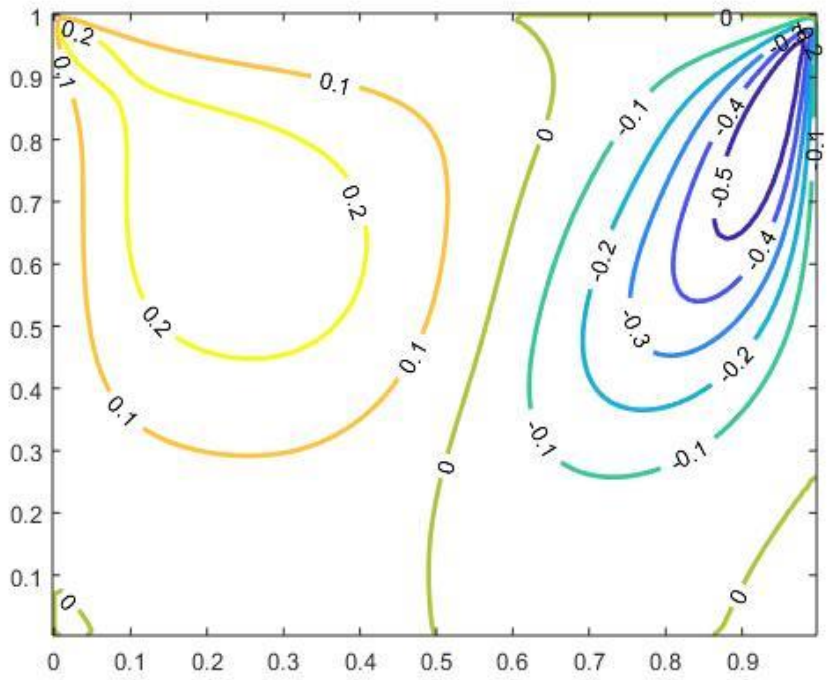

Figure 10. 2D v-velocity contours with various levels for $\upsilon = 0.005$. Grid size 100x100

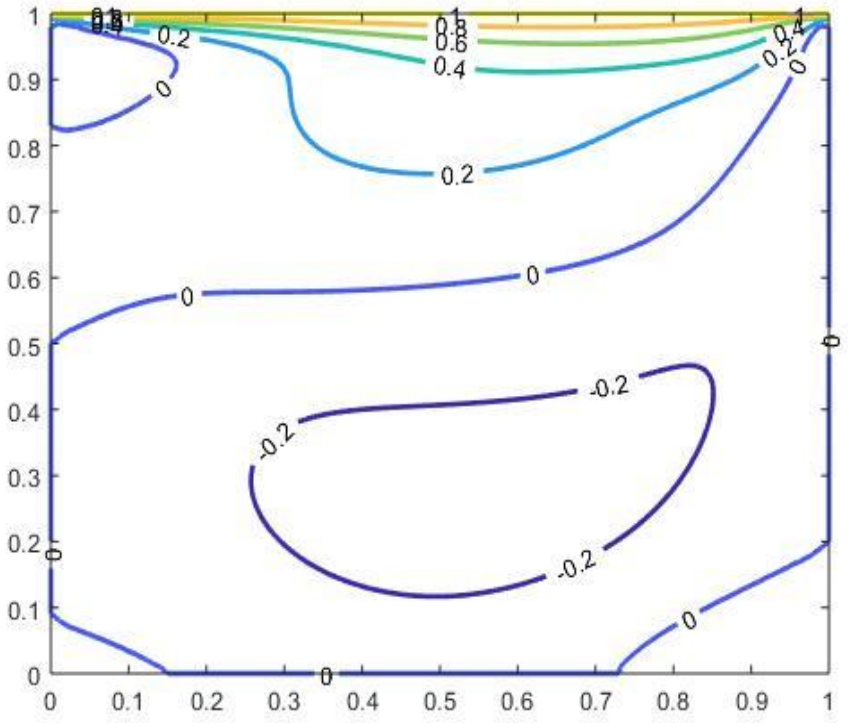

Figure 11. 2D u-velocity contours with various levels for $\upsilon = 0.002$. Grid size 100x100

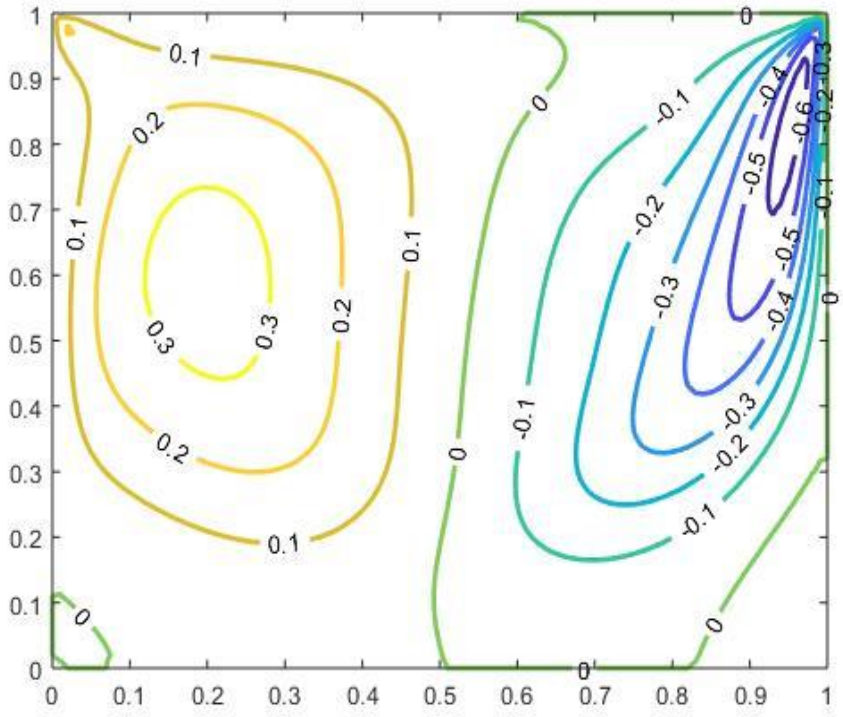

Figure 12. 2D v-velocity contours with various levels for $\upsilon = 0.002$. Grid size 100x100

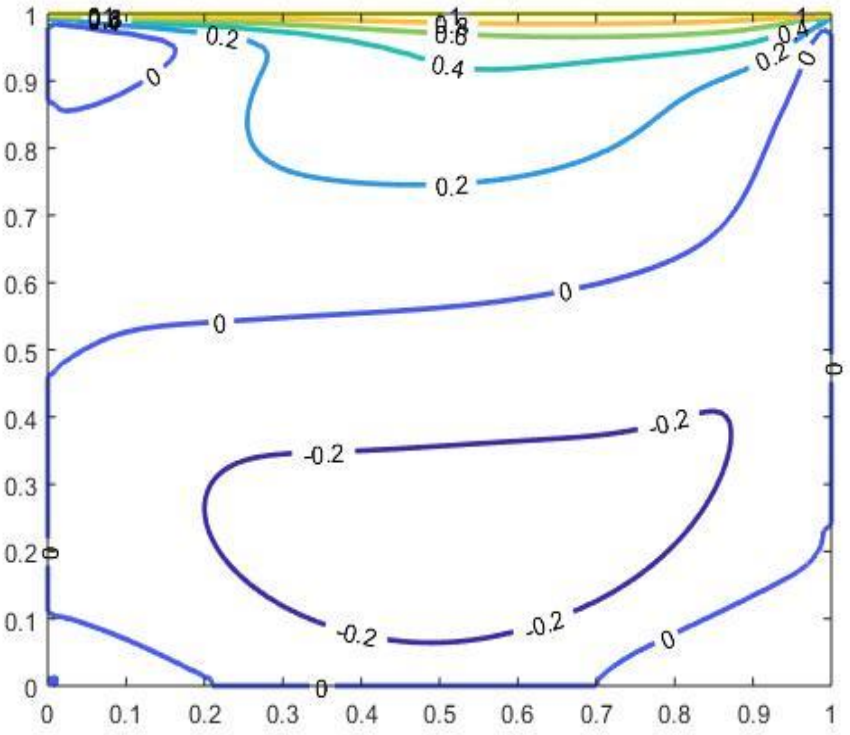

Figure 13. 2D u-velocity contours with various levels for $\upsilon = 0.001$. Grid size 100x100

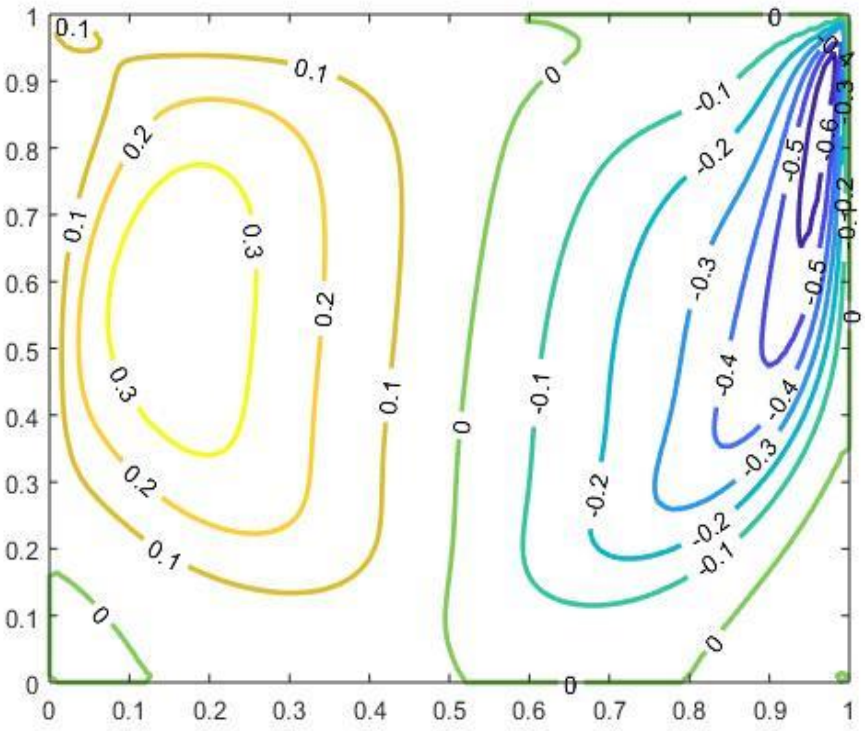

Figure 14. 2D v-velocity contours with various levels for $v = 0.001$. Grid size 100x100

5. Conclusion

The system of steady state Navier-Stokes equations written in velocity pressure form was solved using a finite difference method constructed by using fourth order central difference approximations for the derivatives. It was shown to be efficient and stable than existing lower order methods for various viscosity coefficients. 2D constant velocity curves were plotted to illustrate the flow graphically.

The system of Navier-Stokes equations written in stream-vorticity form has better structure than the primitive system solved in this paper and by analyzing the stream function and vorticity functions, one could expect to get better insight into the motion of the viscous flow. We have developed a numerical method to solve the system of Navier-Stokes equations written in stream-vorticity form and are currently testing the method.

We plan to extend our research work to cover the flow of a non-Newtonian fluid. A non-Newtonian fluid is a fluid that does not follow Newton's law of viscosity, i.e., constant viscosity independent of stress. In non-Newtonian fluids, viscosity can change when under force to either more liquid or more solid. Ketchup, for example, becomes runnier when shaken and is a non-Newtonian fluid. In fact, many fluids around us are non-Newtonian fluids and study of the flow of such fluids are at utmost interest for the researchers.

The system of equations that govern the flow of a non-Newtonian fluid is very similar to the system we have provided in this article. In reality, most fluids are non-Newtonian, which means that their viscosity dependent on strain-rate. We are in the process of studying the flow in a long duct such as a pipe and we expect to achieve better results than those exist from our method described in this article with suitable modifications.

Acknowledgments

The authors would like to thank the reviewers for their valuable suggestions and comments to improve the presentation of this paper.

REFERENCES

Abdallah, S. (1987). Numerical Solutions of the pressure Poisson Equation with Neumann Boundary Conditions Using a Non-Staggered Grid, Journal of Computational Physics, pp.182-192.

Armfield, S.W. (1991). Finite Difference Solutions of the Navier-Stokes Equations on Staggered and Non-Staggered grids, Computers & Fluids, Pergamon Press, pp 1 – 17.

Barragy, E. and Carey, G.F. (1997). Stream function-vorticity driven cavity solution using p finite elements, Computers & Fluids, Vol. 26, pp. 453-468.

Boppana, V. and Gajjar, J. (2010). Global flow instability in a lid-driven cavity, International Journal of Numerical Methods in Fluids, pp. 827-853

Botella, O. and Peyret, R. (1998). Benchmark spectral results on the lid-driven cavity flow, Computers & Fluids, Vol. 27, pp. 421-433.

Bruneau, C.H. and Saad, M. (2006). The 2D lid-driven cavity problem revisited, Computers & Fluids, Vol. 35, pp. 326-348.

Choo, J. Y. and Schultz, D. (1994). A High Order Difference Method for the Steady State Navier-Stokes Equations, Computer Mathematics and Applications Vol. 27, No 11, pp105 – 119.

Chorin, A. J. (1968). Numerical Solutions of the Navier-Stokes Equations. Mathematics and Computers, pp. 745 – 762.

Dubas, S, M. (2001). A High order Scheme for Driven Cavity Problem, International Journal for Applied Science and Computations, Vol 8, No. 3, pp 155 – 170.

Galdi, G.P. (2011). *An Introduction to the Mathematical Theory of the Navier-Stokes Equations Steady – State Problems,* Springer Monographs in Mathematics, pp 1 – 21.

Greenspan, D. and Casulli, V. (1988). *Numerical Analysis for Applied Mathematics, Science and Engineering,* Addison-Wesley Publishing Company.

Hassanien, I.A., Salama, A.A., and Hosham, H.A. (2005). Fourth-order finite difference method for solving Burger's equation, Applied Mathematics and Computation, Vol. 170, pp 781–800.

Khorasanizade, S. and Sousa, J. M. (2014). A detailed study of lid-driven cavity flow at moderate Reynolds numbers using Incompressible SPH, International Journal of Numerical Methods in Fluids, Vol. 76, pp. 653-668

LeVeque, R. J. (2007). *Finite Difference Methods for Ordinary and Partial Differential Equations*, Society for Industrial and Applied Mathematics.

Liu J. and Wang C. Y. (2019). Closed-Form Solutions of Unsteady Two-Fluid Flow in a Tube, Applications and Applied Mathematics, Vol. 14, Issue 1, pp. 586-601.

Magalhães, J. P., Albuquerque, D. M., Pereira, J. M. and Pereira, J. C. (2013) Adaptive mesh finite-volume calculation of 2D lid-cavity corner vortices, Journal Computational Physics, Vol. 243, pp. 365-381

Osman, A., Schultz, D. and Dubas, S. (2008) "Comparison of Methods for Viscous, Incompressible Flows in a Channel with a Step", International Journal for Applied Science & Computations, vol 15, No. 1, pp. 41-52.

Wang, C.Y. (2017). Starting flow in a channel with two immiscible fluids, Journal of Fluids Engineering, Vol. 139(12), #124501.

Zhang, J. (2003). Numerical simulation of 2D square driven cavity using fourth-order compact finite difference schemes, Computers and Mathematics with Applications, Vol. 45, pp. 43-52.

Zogheib, B. and Barron, R. M. (2011). Velocity–pressure coupling in finite difference formulations for the Navier-Stokes equations, International Journal for Numerical Methods in Fluids, Vol. 65, No. 9, pp1096 – 1114.